ACS APPLIED MATERIALS & INTERFACES

Research Article

www.acsami.org

Highly Sensitive Wide Bandwidth Photodetector Based on Internal Photoemission in CVD Grown p-Type MoS_2/Graphene Schottky Junction

PhaniKiran Vabbina,*[,†] Nitin Choudhary,[‡] Al-Amin. Chowdhury,[†] Raju Sinha,[†] Mustafa Karabiyik,[†] Santanu Das,[‡] Wonbong Choi,[‡] and Nezih Pala*[,†]

[†]INSYST Laboratory, Electrical and Computer Engineering, Florida International University, Miami, Florida 33174, United States

[‡]Nanomaterials and Device Laboratory, Department of Materials Science and Engineering, University of North Texas, Denton, Texas 76207, United States

Supporting Information

ABSTRACT: Two dimensional (2D) Molybdenum disulfide (MoS_2) has evolved as a promising material for next generation optoelectronic devices owing to its unique electrical and optical properties, such as band gap modulation, high optical absorption, and increased luminescence quantum yield. The 2D MoS_2 photodetectors reported in the literature have presented low responsivity compared to silicon based photodetectors. In this study, we assembled atomically thin p-type MoS_2 with graphene to form a MoS_2/graphene Schottky photodetector where photo generated holes travel from graphene to MoS_2 over the Schottky barrier under illumination. We found that the p-type MoS_2 forms a Schottky junction with graphene with a barrier height of 139 meV, which results in high photocurrent and wide spectral range of detection with wavelength selectivity. The fabricated photodetector showed excellent photosensitivity with a maximum photo responsivity of 1.26 AW^{-1} and a noise equivalent power of 7.8×10^{-12} W/$\sqrt{Hz}$ at 1440 nm.

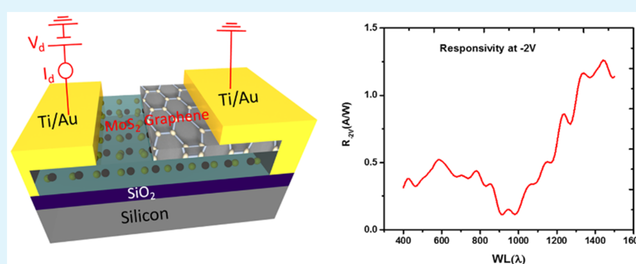

KEYWORDS: *atomic layer MoS_2, graphene, Schottky junction, 2D hybrid materials, photodetector, CVD*

1. INTRODUCTION

Graphene, a semimetallic, two-dimensional (2D) material with a single atomic layer, has been the most widely researched material owing to its superior electrical, mechanical, and optical properties such as high carrier mobility (~200 000 $cm^2V^{-1}s^{-1}$), high mechanical strength, flexibility, transparency, and high absorption rate (2.30% of incident light per each layer) among many other properties.[1,2] Further, the gapless nature of graphene enables charge carrier generation over a wide energy spectrum from ultraviolet (UV) to terahertz (THz), making it a unique material for photonics and optoelectronics applications.[3] Making use of the unique capabilities of graphene, many studies have been performed over the past decade to demonstrate highly efficient graphene photodetectors (GPDs) from visible to infrared (IR) range.[4−6] Despite the many favorable properties, factors such as low total absorption due to single layer nature of graphene limited the responsivity of conventional GPDs to few tens of mAW^{-1}.[3] Alternative methods such as colloidal quantum dots, microcavities, or plasmonic nanostructures have been used to improve the responsivity of the GPDs but these devices were found to respond to very limited spectra of the incident light.[7] However, 2D semiconductor transition metal dichalcogenides (sTMDs) have also been widely used for photodetector applications.[8] Atomically thin sTMDs provide a wide range of advantages in optoelectronics when compared to their bulk counterparts owing to their high transparency, flexibility, and tunable bandgap. In particular, MoS_2 is a unique semiconductor material whose bulk counterpart has an indirect-gap of 1.20 eV but when reduced to a monolayer, it changes into direct bandgap material with a bandgap of 1.80 eV due to quantum confinement. This results in higher absorption coefficient and efficient electron−hole pair generation under photo excitation in monolayer MoS_2. A 10^4 fold enhancement of luminescence quantum yield for monolayer MoS_2 compared to bulk MoS_2 has been observed.[9] There are several reports on the fabrication of MoS_2-based photodetectors. The first phototransistor based on monolayer MoS_2 showed a relatively poor photo responsivity of 7.50 mAW^{-1}.[10] Choi et al. used multilayer MoS_2 to achieve 100 mAW^{-1} photo responsivity,[11] showing an improvement over the first phototransistor but still low compared to GPDs. Since then, much progress has been made, and more recently, phototransistors with responsivities ranging from few hundreds of mAW^{-1} to hundreds of AW^{-1} were reported.[12,13] However, the reported MoS_2-based photo-

Received: January 29, 2015
Accepted: July 6, 2015
Published: July 6, 2015

 © 2015 American Chemical Society

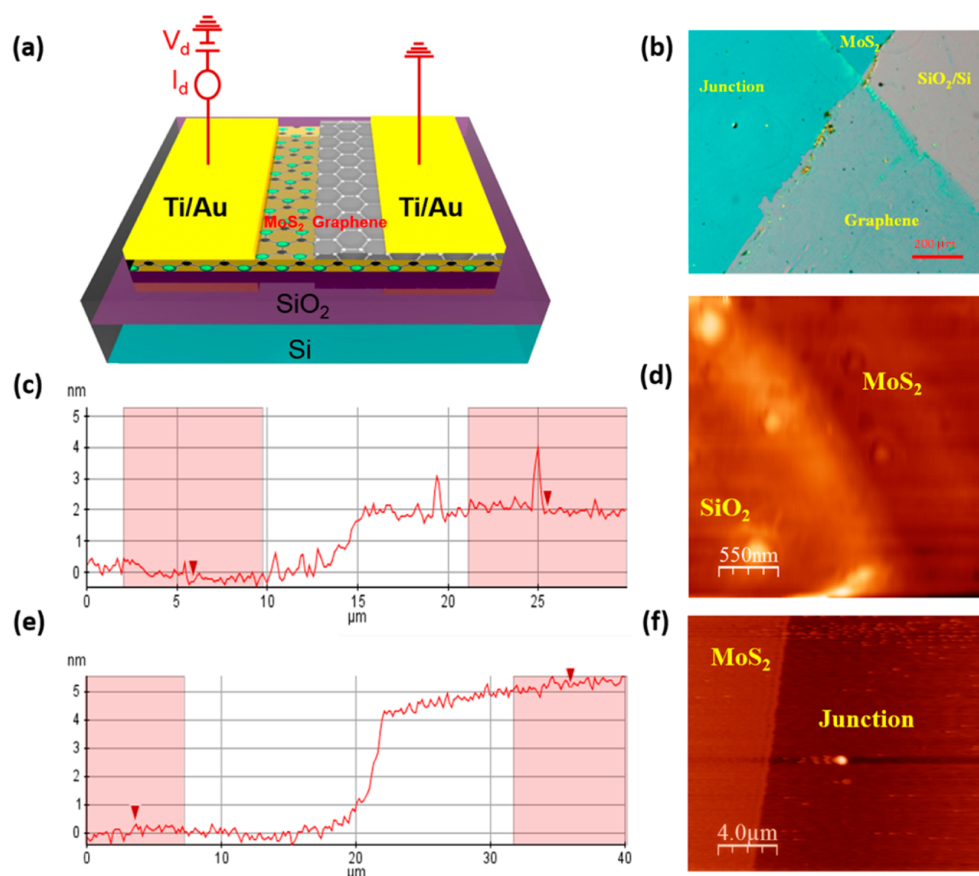

Figure 1. (a) Schematic of p-type MoS_2/graphene junction device; (b) optical image of MoS_2/graphene junction with individual areas clearly visible; (c) AFM height profile showing height of MoS_2; (d) AFM image of MoS_2−SiO_2 interface; (e) thickness of graphene at MoS_2/graphene junction; and (f) AFM image of MoS_2/graphene junction.

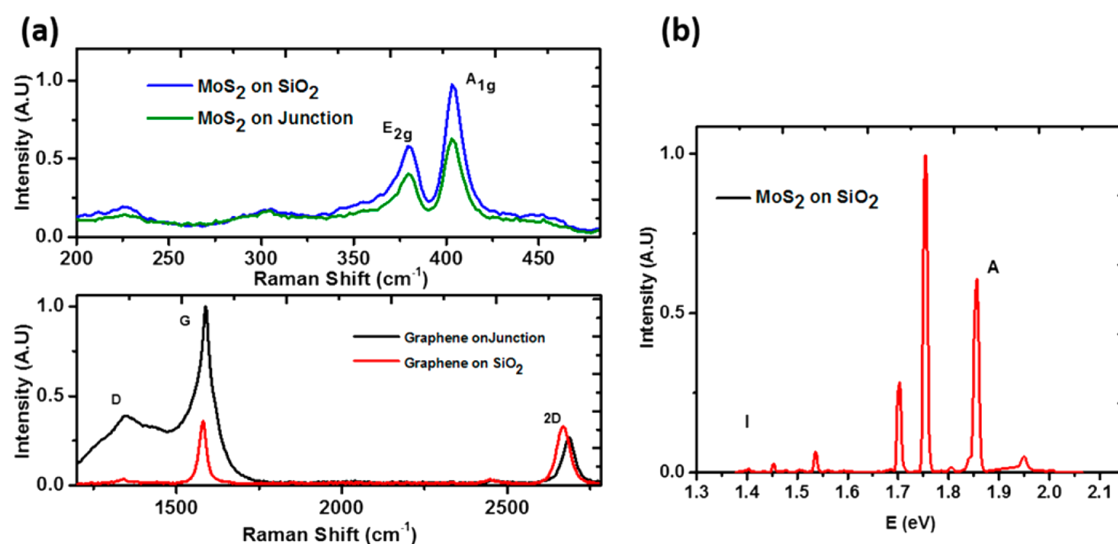

Figure 2. (a) Raman spectrum of MoS_2 and Graphene on SiO_2 and junction and (b) photoluminescence of MoS_2 on SiO_2 showing sharp peaks at 1.7, 1.75, and 1.85 eV, and smaller ones at 1.4 and 1.55 eV.

detectors are limited by narrow wavelength range and long response times.

To further improve the properties of graphene and MoS_2-based photodetectors, it is imperative to design new device structures like composites, heterostructures, or functionally graded thin films. Numerous efforts have been made to combine the properties of TMDs and graphene by assembling graphene with other 2D crystals to create multifunctional high-performance hybrid devices.[14−20] One of the hybrid structures includes the combination of graphene and MoS_2 in the form of thin film heterostructures. Coupling graphene with MoS_2 can produce a hybrid material that can utilize the high photon absorption capability in MoS_2 and high electron mobility in graphene to realize a highly efficient photodetector as shown by

DOI: 10.1021/acsami.5b00887
ACS Appl. Mater. Interfaces 2015, 7, 15206−15213

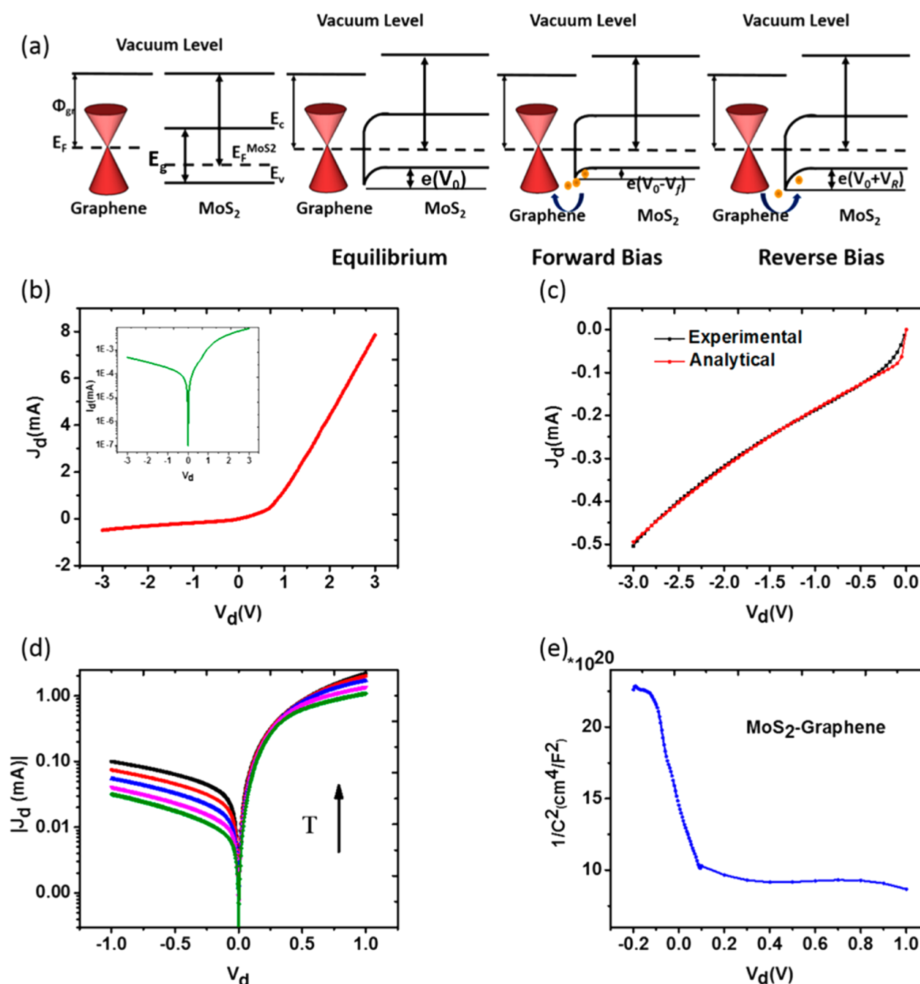

Figure 3. (a) Energy level alignment for MoS_2/ graphene structure, band diagram at junction in equilibrium, forward bias and reverse bias with carrier flow; (b) *J*−*V* curve showing rectification under reverse bias and exponentially increasing current in forward bias (inset: Absolute value of *J*−*V* plotted in logarithmic scale); (c) *J*−*V* at different temperatures showing an increase in *J* with increase in temperature; (d) $1/C^2$ plotted against voltage; and (e) reverse current from experimental and analytical model.

Zhang et al., who have achieved a high responsivity of 1.2×10^7 A/W by applying a gate voltage of −10 V at 690 nm laser illumination by simply stacking n-type monolayer MoS_2 over graphene.[21] In the present study, we assembled few layers of graphene with few layers of p-type MoS_2 to form a simple MoS_2/graphene Schottky junction photodiode. We found that p-type MoS_2 provides a much lower Schottky barrier height with graphene with a broad spectral range of detection.

2. RESULTS AND DISCUSSION

Figure 1a shows the schematic of the studied photodiode. Sputtering-CVD technique was used to synthesize a few layers of MoS_2, as described by Choi et al.,[22] while the CVD process is used to synthesize graphene.[23] Figure 1b shows the optical microscope image depicting the color contrast over the four different regions: (1) SiO_2, (2) MoS_2, (3) Graphene, and (4) MoS_2/graphene junction (MGJ). Atomic force microscopy (AFM) was used to study the thickness and the interface of MoS_2 and graphene. Figure 1, parts c and e, shows the thickness measured using AFM. We observed that the average thickness of MoS_2 layer is 2 nm and that of graphene is 5 nm, which suggests that as-grown MoS_2 was about 3−4 layers thick. Raman spectroscopy is a widely used method to determine the number of layers, quality and defects present in these 2D materials.[24]

Figure 2a shows the Raman spectra of MoS_2 and graphene, measured over SiO_2 and junction regions using a 532 nm excitation laser line. We observed strong peaks at 379.77 and 403.52 cm^{-1}, corresponding to the in plane E^1_{2g} mode and out-of-plane A_{1g} mode of MoS_2, respectively. The peak frequency difference of 23.75 cm^{-1} between the two modes indicates that as-grown MoS_2 is 4−5 layers thick, which is in agreement with the previously reported results[25] and also with our results obtained by AFM height analysis. The Raman spectra of graphene on SiO_2 evidence the formation of 2D and "G" characteristics peaks at 2666.83 and 1580.16 cm^{-1}, respectively, which is consistent with the previous reports on few layer graphene.[26] However, a red peak shift of ∼18.8 cm^{-1} was observed in the 2D peak of graphene when Raman spectra was taken at the junction. The observed peak shift could be attributed to an increase in hole concentration at the MoS_2/graphene junction.[27] This is a common phenomenon for p-type semiconductor-metal Schottky junction where holes travel from the p-type semiconductor to metal as their Fermi levels are aligned. Figure 2b shows photoluminescence (PL) spectrum measured at room temperature. Peak "A" associated with excitonic transitions at the "K" point of Brillouin zone is

DOI: 10.1021/acsami.5b00887
ACS Appl. Mater. Interfaces 2015, 7, 15206−15213

observed at 1.85 eV while peak "I" at 1.40 eV corresponding to indirect gap which is prominent in bulk MoS_2 is almost negligible, confirming that the fabricated device is formed by few layers of MoS_2.[28,29] We also observe a strong emission at 1.75 eV which has been attributed to radiative recombination of neutral excitons bound to defects (X^0) caused by Sulfur (S) vacancies.[30,31]

The conduction behavior of MoS_2 films deposited on Si/SiO_2 substrates was determined by fabricating field effect transistor (FET) devices with 50 nm thick Au as source and drain electrodes, 300 nm thick SiO_2 served as the dielectric layer, while doped silicon was used as the back gate. The output and transfer characteristics of our MoS_2 FET, as shown in Figure S1 in the Supporting Information (SI), confirm a p-type conduction behavior with a field effect mobility of ~12.24 $cm^2V^{-1}s^{-1}$, which is higher than mechanically exfoliated and CVD grown MoS_2 FETs on Si/SiO_2 substrates[32,33] and $I_{on/off}$ ratio of ~10^6.[22] The origin of p-type conduction in MoS_2/SiO_2 system is not fully understood yet. On the basis of ab initio DFT calculations. Douli et al. showed that a p-type conduction in MoS_2 films on SiO_2 substrates could be due to the presence of localized trap states arising from impurities or defects within the oxide substrate or at the interface with the conducting channel. Such states can redefine the effective Fermi level of the hybrid system to make it either n-type or p-type. The effect of the trap states could be especially pronounced in low dimension materials, as in the case of few layer MoS_2.[34] The trap states might have originated from the immobile ionic charges, SiO_2 surface oxygen dangling bonds or foreign impurities presented at the SiO_2/MoS_2 interface during MoS_2 synthesis. The defects present at the SiO_2 and MoS_2 interface could also be due to the Mo diffusion into SiO_2 when it was sulfurized in the CVD furnace at the high temperature of 600 °C.[35,36]

When a semimetallic graphene is assembled over semiconducting MoS_2, a Schottky junction like behavior is expected. The schematic of carrier transport at MoS_2/graphene junction under forward and reverse bias is shown in Figure 3a. In Figure 3b, the current−voltage ($J-V$) characteristics measured at MoS_2/graphene is displayed. As can be seen from the $J-V$ plot and the |log (J)| vs V plot shown in the inset, the junction shows a clear rectification as exponentially increasing current passes in the forward bias, while there is strong resistance in the reverse bias, which prevents flow of holes from graphene to MoS_2. From the current−voltage and the Raman measurement results showing an influx of holes in to graphene from MoS_2 at the junction, it can be concluded that a Schottky barrier junction (SBJ) similar to a metal−semiconductor junction is formed between graphene and MoS_2. However, we observe that the current never reaches a complete saturation in reverse bias unlike an ideal metal−semiconductor Schottky junction. This is due to the bias dependent Fermi level observed in graphene which results in a variable Schottky barrier height (SBH) at different bias voltages. Recently Tongay et al. have proposed a model for the current observed in graphene−semiconductor junctions taking into account the change in graphene Fermi level with applied bias.[37] The current in the Schottky diode is given by the following:

$$J(V) = A^*T^2\exp\left(-\frac{e\Phi^0{}_{SBH} + e\Delta\Phi_{SBH}(V)}{k_BT}\right)\left[\exp\left(\frac{eV}{k_BT}\right) - 1\right] \quad (1)$$

where A^* is Richardson's constant, Φ^0_{SBH} is Schottky barrier height (SBH) at zero bias and $e\Delta\Phi_{SBH}(V)$ is the difference in Schottky barrier height due to change in the Fermi level of Graphene with applied bias and is given by the following:

$$e\Delta\Phi_{SBH}(V) = -(\Delta E_F^G(V)) = \hbar V_F[\sqrt{\pi(n_0 - n_{induced})} - \sqrt{\pi n_0}] = -\frac{1}{2}\hbar v_F\sqrt{\frac{\pi\varepsilon_s\varepsilon_0 N_A(V_0 + V_R)}{2en_0}} \quad (2)$$

where N_A is acceptor concentration in the semiconductor, V_0 is the built-in voltage, V_R reverse bias voltage, and n_0 the carrier density in graphene. The modified saturation current is as follows:

$$J_s(V) = A^*T^2\exp\left(-\frac{e\Phi^0{}_{SBH} + e\Delta\Phi_{SBH}(V)}{k_BT}\right) \quad (3)$$

Zero bias Schottky barrier height (Φ^0_{SBH}) was measured from the temperature dependent $J-V$ measurements carried at four different temperatures and capacitance−voltage ($C-V$ measurements were used to measure acceptor concentration N_A and built in voltage V_0. The change in current (|J|) with temperature is shown in Figure 3c, which shows that the current increases with temperature in both bias directions. The value of Φ^0_{SBH} can be obtained from the slope of Richardson's plot given by the following:[38,39]

$$\Phi^0{}_{SBH} = \frac{V_1}{n} - \frac{k}{q}\frac{\partial[\ln(I/T^2)]}{\partial(1/T)} \quad (4)$$

We measured the Φ^0_{SBH} of MGJ at V_1= 0.3 V to be 139.20 meV, where the ideality factor "n" is obtained from intercept of the linear region of the $J-V$ plot and measured to be 1.86 while Richardson's constant A^* is 0.70 × 10^{-6} A cm^{-2} K^{-2}. The greater than unity value of the ideality factor can be attributed to enhanced image-force lowering across the MGJ and Schottky-barrier inhomogeneity.[37] Capacitance−Voltage measurements are used to obtain built−in voltage (V_0) and doping density values, from Schottky−Mott relationship. When square of inverse of capacitance ($1/C^2$ (cm^4F^{-2})) plotted against applied voltage in reverse bias, ($1/C^2$) varies linearly with applied bias before saturating this can be extrapolated to intersect the abscissa to obtain built-in potential $V_0 = (\Phi_{MoS_2} - \Phi_{Gr})$, and the slope of the linear region gives the doping density (N_A) of MoS_2. From Figure 3d, we can see that the measured values hold the linearity in reverse bias. We measured V_0 and N_A values to be 280 mV and 6.64 × 10^{21} cm^{-3} (3.32 × 10^{15} cm^{-2}) respectively. By considering the work function of graphene from literature to be 4.50 eV, the work function of p-type MoS_2 is found to be 4.78 eV.[40] Experimental and theoretical values of reverse current obtained from the analytical model developed shown in Figure 3e closely match each other.

One of the most interesting application of Schottky diodes is their use as photodetectors. MoS_2/graphene hybrid structure would be an excellent material for photodetection, as both

DOI: 10.1021/acsami.5b00887
ACS Appl. Mater. Interfaces 2015, 7, 15206−15213

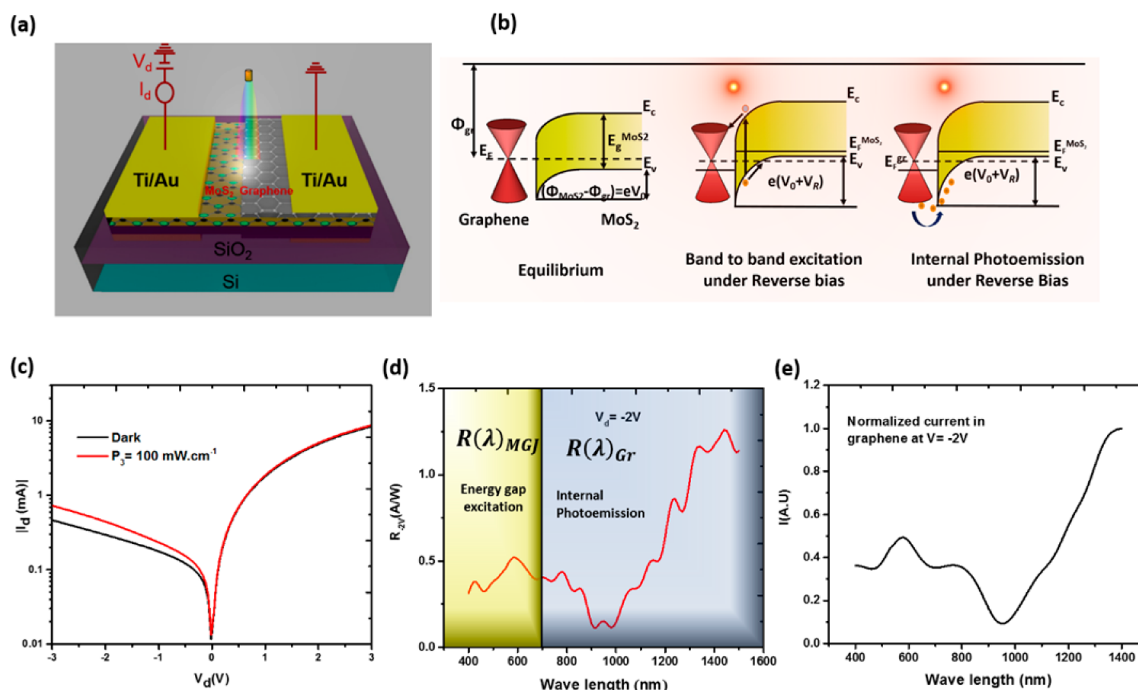

Figure 4. (a) MGPD under illumination; (b) illustration of photocurrent generation in a Schottky diode under illumination; (c) $J-V$ at dark and under 100 mW/cm^2 illumination; (d) photo responsivity of MGPD at different wavelengths (spectral response); and (e) photoconductivity of graphene.

materials show high photosensitivity. Graphene being a gapless material exhibits sensitivity to light over a wide range of wavelengths from visible light to mid and far-infrared. High electron mobility and high absorption would also contribute toward high responsivity in graphene. However, atomically thin MoS_2 has shown some interesting optical phenomenon such as 10^4 fold increase in photoluminescence when compared to bulk MoS_2 and significant responsivity in visible light.[29] By stacking both MoS_2 and graphene together to form Schottky junction, we would be able to harness these features of both materials to build high performing photodetectors. In general, Schottky photodiodes operate in two modes: (1) Energy gap excitation where electron−hole pairs are generated by band to band excitation in the semiconductor when energy of photon is greater than the band gap of semiconductor $h\nu > E_g$ and (2) internal photoemission which is observed when the incident light energy is greater than the Schottky barrier energy and smaller than the bandgap of semiconductor ($\Phi_{SBH} < h\nu < E_g$) resulting in photo emission of carriers from metal surface close to the junction which are then driven toward the semiconductor over the Schottky barrier due to the electric field in the junction. This leads to a wide spectral range of detection based on the SBH values obtained.[41] Both schemes are explained in Figure 4b. A Schottky barrier photodiode is conventionally operated in reverse bias where the increase in barrier results in very small reverse current and hence any increase in current by the photocurrent can be detected with a high sensitivity. This makes it easy to exactly measure the photocurrent generated. The expression for diode current is given by the following:

$$J(V) = A^{*}T^{2}\left[\exp\left(\frac{eV}{k_{B}T}\right) - 1\right] - J_{op} \tag{5}$$

where J_{op} is the photon induced current equal to $R^{*}P_{op}$, where R is the responsivity of the photodiode, and P_{op} is the power of incident light, the first part of the equation is the current equation in ideal Schottky diode. By replacing the diode current term with the modified Schottky diode current presented in eq 1, we can write the diode current equation as follows:

$$J(V) = A^{*}T^{2}\exp\left(-\frac{e\Phi^{0}{}_{SBH} + e\Delta\Phi_{SBH}(V)}{k_{B}T}\right)\left[\exp\left(\frac{eV}{k_{B}T}\right) - 1\right] - J_{op} \tag{6}$$

In order to study the operation of the photodiode in both modes we have studied the performance of the device in a wide spectral range from 400 to 1500 nm. The spectral response "R" of the device measured at 2 V reverse bias is shown in Figure 4d. When the diode is operated in energy gap excitation mode where $h\nu > E_g^{MoS_2}$ a maximum photo responsivity of $R_{max} = 0.52$ AW^{-1} is observed at 590 nm. Beyond 670.00 nm, where the incident photon energy is smaller than $E_g^{MoS_2}$ the photo current is due to internal photo emission in Graphene where photo generated holes move toward MoS_2. We find that the responsivity actually increases from 980 nm reaching a maximum value of 1.26 AW^{-1} at 1440 nm before starting to fall. The obtained responsivity is not the highest but higher than many state of the art devices. A comparison of the MoS_2/graphene photo detectors is provided in Table 1 of the SI. This increase in responsivity follows the increase in photoconductivity observed in graphene which is shown in Figure 4(e). This kind of increased optical conductivity in graphene has been observed in intra band conductivity in earlier studies.[42]

One of the most important detector characteristics is the noise equivalent power (NEP), which represents the lowest

DOI: 10.1021/acsami.5b00887
ACS Appl. Mater. Interfaces 2015, 7, 15206−15213

input power giving a unit signal/noise ratio. In a Schottky junction photodetector, both Johnson noise which is due to thermal noise associated with the resistance and shot noise, which is associated with the overall current contribute toward the overall noise. The Johnson noise current i_j is given by $i_j = ((4k_BT)/(R_{eq}))^{1/2}$ where k_B is the Boltzmann constant, T is the absolute temperature, and R_{eq} is the equivalent resistance. The R_{eq} is obtained from the slope of $I-V$ of MGPD at −2 V measured in dark. For R_{eq} of 5.83 MΩ and for normalized bandwidth (B) at room temperature the Johnson noise i_j is 1.68 pA. The shot noise is given by the following:

$$i_s = \sqrt{2q(I_{ph} + I_d)B}$$

where I_{ph} is the photo current, and I_d is the dark current. The measured shot noise current at −2 V is 11.2 pA at 1400 nm. The total noise current i_n is 11.3 pA, and the NEP, which is the ratio of i_n and the responsivity, is calculated.[43,44] We obtain a minimum NEP of 7.8×10^{-12} W/$\sqrt{}$Hz and corresponding detectivity of 4.2×10^{10} cm. $\sqrt{}$ Hz/W at 1400 nm. The measured NEP of MGPD is less than typical Si photodetectors.

3. CONCLUSIONS

In summary, we succeeded in fabricating high bandwidth photodetectors by stacking a few layers of p-type MoS_2 over a few layers of graphene to form a Schottky junction photodiode. Stable optical properties of MoS_2 and high carrier mobility in graphene contribute to efficient charge separation at the junction. Apart from the impressive charge carrier properties, graphene also exhibits a wide bandwidth absorption, which allows for the photodiode to operate in both energy gap excitation mode and internal photo emission mode, thereby extending the detection range to higher wavelengths than those reported in earlier MoS_2/graphene Schottky junctions. From the spectral response, we find that the fabricated device performs well over a wide range of wavelengths from visible region to mid infrared region with internal photo emission in graphene playing a major role in extending the range of the device. We have studied the junction characteristics and presented the underlying phenomenon of charge transfer in a 2D MoS_2/graphene Schottky junction. The CVD process is used in growing large area MoS_2 and graphene which, along with the simplicity of fabrication, can be easily integrated with metal oxide semiconductor (CMOS) technology.

4. EXPERIMENTAL SECTION

4.1. Fabrication. MoS_2/graphene junction devices were fabricated by growing atomically thin MoS_2 film on Si/SiO_2 substrates followed by the transfer of graphene. For MoS_2 deposition, the first step involves the sputtering of Mo thin films on (100) oriented *n*-type (As doped, resistivity <0.005 Ω.cm) silicon substrates coated with 300 nm thick SiO_2 layer. A high purity (99.99%) Mo metal target of 50 mm diameter was used for sputtering Mo thin films. In the second step, magnetron sputtered Mo/SiO_2/Si films were subsequently placed in a low-pressure chemical vapor deposition (LPCVD) system (Graphene Square CVD) and sulfurization was proceeded at 600 °C for 30 min. The detail of MoS_2 synthesis can be found in our recent report.[22] Polycrystalline copper foils (Nimrod Hall, 99.9% purity, 25 μm thick) were used as the substrates for graphene growth. The Cu foil was electro-polished using a home-built electrochemistry cell, rinsed in methanol and deionized water solution (1:1), and then gently blown with compressed nitrogen for drying. The cleaned Cu foil was loaded into the low-pressure thermal CVD system. The reaction chamber was evacuated to ∼0.1 mTorr and refilled with 2.5 sccm of pure H_2. The temperature was increased to 1000 °C within 40 min and then annealed for 1 h. After annealing, 20 sccm of CH_4 and 2.5 sccm of H_2 were introduced into the chamber for graphene growth at 1000 °C under the pressure of 5 Torr for a certain growth time. After the growth, the CH_4 flow was turned off, and the chamber was cooled down under H_2 environment.

The graphene transfer method used was as follows: (1) PMMA (MicroChem Corp. 495 PMMA A2) solution was spin-coated onto the graphene/Cu foil at 5000 rpm for 1 min, followed by drying the sample in the air; (2) the Cu foil was etched with metal etchant (type I, Transene company, Inc.), resulting in the PMMA/graphene film floating to the top of the etchant solution; (3) the PMMA/graphene film was washed in a beaker containing deionized water, and floated on 10% HCl solution for 10 min, and transferred to a beaker with deionized water for another wash (done 3×); (4) the film was transferred to a beaker with deionized water for another wash, and this process was repeated three times; (5) the film was then finally scooped onto a Si/SiO2/MoS_2 substrate with the PMMA side up and dried in the air; (6) the PMMA layer was removed by immersing the sample in a large volume of acetone; and (7) the sample was dried with compressed nitrogen. Figure 1a shows the schematic of the MoS_2/graphene photodetector device structure simply formed by a manual stacking of a graphene onto MoS_2. 50-nm thick Au/Ti metal contacts were deposited by electron beam evaporation after using a shadow mask. The shadow masks were carefully prepared using a laser writer so as to maintain the contact area and position accurately. The deposited contacts were later annealed at 350 °C for 30 min.

4.2. Characterization. Atomic force microscopy (Parks NX-10) and Raman spectroscopy (Bay Spec spectrometer) were employed to measure the thickness of MoS_2 and graphene layers. In order to determine the conduction in MoS_2, electrical measurements were performed at room temperature using an Agilent B2912A precision source/measure unit (2 ch, 10 fA, 210 V, 3A DC/10.5A Pulse) connected to a probe station with 20 μm size tungsten probes. Room temperature photoluminescence (PL) using He−Cd laser line at 325 nm and 10 mW laser power, and visible spectroscopy was employed to characterize the quality of MoS_2/graphene heterostructure. The spectral response measurement system QEX10 from PV Measurements Inc. which houses a Xenon arc lamp was used to measure the spectral response of the MoS_2/graphene photodetectors.

The optical power of the xenon lamp at different wavelengths was measured using a multifunction optical meter from Newport. A plot of optical power of the xenon lamp with respect to the wavelength is given in Figure S2 in the SI. The responsivity of the MGPD was calculated by taking the ratio of photocurrent density and power density at every 10 nm between 400 and 1500 nm.

■ ASSOCIATED CONTENT

Supporting Information

Detailed MoS_2 transfer characteristics and the power of xenon lamp with respect to wavelength, and a comparison of fabricated MGPD with other MoS_2. The Supporting Information is available free of charge on the ACS Publications website at DOI: 10.1021/acsami.5b00887.

■ AUTHOR INFORMATION

Corresponding Authors

*E-mail: pvabb001@fiu.edu (P.V.).
*E-mail: npala@fiu.edu (N.P.).

Author Contributions

The manuscript was written through contributions of all authors. All authors have contributed equally and have given approval to the final version of the manuscript.

Notes

The authors declare no competing financial interest.

DOI: 10.1021/acsami.5b00887
ACS Appl. Mater. Interfaces 2015, 7, 15206−15213

■ ACKNOWLEDGMENTS

This work was supported by National Science Foundation CAREER program under Award 0955013. R.S. gratefully acknowledges the financial support provided through a presidential fellowship by the University Graduate School (UGS) at Florida International University.

■ REFERENCES

(1) Xia, F.; Mueller, T.; Lin, Y.; Valdes-Garcia, A.; Avouris, P. Ultrafast Graphene Photodetector. *Nat. Nanotechnol.* **2009**, *4*, 839−843.

(2) Kang, C. G.; Lee, S. K.; Yoo, T. J.; Park, W.; Jung, U.; Ahn, J.; Lee, B. H. Highly Sensitive Wide Bandwidth Photodetectors Using Chemical Vapor Deposited Graphene. *Appl. Phys. Lett.* **2014**, *104*, 161902.

(3) Bonaccorso, F.; Sun, Z.; Hasan, T.; Ferrari, A. Graphene Photonics and Optoelectronics. *Nat. Photonics* **2010**, *4*, 611−622.

(4) Lemme, M. C.; Koppens, F. H.; Falk, A. L.; Rudner, M. S.; Park, H.; Levitov, L. S.; Marcus, C. M. Gate-Activated Photoresponse In A Graphene P−N Junction. *Nano Lett.* **2011**, *11*, 4134−4137.

(5) Pospischil, A.; Humer, M.; Furchi, M. M.; Bachmann, D.; Guider, R.; Fromherz, T.; Mueller, T. Cmos-Compatible Graphene Photodetector Covering All Optical Communication Bands. *Nat. Photonics* **2013**, *7*, 892−896.

(6) Liu, C.; Chang, Y.; Norris, T. B.; Zhong, Z. Graphene Photodetectors with Ultra-Broadband and High Responsivity at Room Temperature. *Nat. Nanotechnol.* **2014**, *9*, 273−278.

(7) Withers, F.; Bointon, T. H.; Craciun, M. F.; Russo, S. All-graphene photodetectors. *ACS Nano* **2013**, *7*, 5052−5057.

(8) Koppens, F.; Mueller, T.; Avouris, P.; Ferrari, A.; Vitiello, M.; Polini, M. Photodetectors Based on Graphene, other Two-Dimensional Materials and Hybrid Systems. *Nat. Nanotechnol.* **2014**, *9*, 780−793.

(9) Mak, K. F.; Lee, C.; Hone, J.; Shan, J.; Heinz, T. F. Atomically Thin Mos 2: A New Direct-Gap Semiconductor. *Phys. Rev. Lett.* **2010**, *105*, 136805.

(10) Yin, Z.; Li, H.; Li, H.; Jiang, L.; Shi, Y.; Sun, Y.; Lu, G.; Zhang, Q.; Chen, X.; Zhang, H. Single-Layer Mos2 Phototransistors. *ACS Nano* **2011**, *6*, 74−80.

(11) Choi, W.; Cho, M. Y.; Konar, A.; Lee, J. H.; Cha, G.; Hong, S. C.; Kim, S.; Kim, J.; Jena, D.; Joo, J. High-Detectivity Multilayer MoS2 Phototransistors with Spectral Response from Ultraviolet to Infrared. *Adv. Mater.* **2012**, *24*, 5832−5836.

(12) Tsai, D.; Liu, K.; Lien, D.; Tsai, M.; Kang, C.; Lin, C.; Li, L.; He, J. Few-layer MoS2 with High Broadband Photogain And Fast Optical Switching For use In Harsh Environments. *ACS Nano* **2013**, *7*, 3905−3911.

(13) Lopez-Sanchez, O.; Lembke, D.; Kayci, M.; Radenovic, A.; Kis, A. Ultrasensitive Photodetectors Based on Monolayer Mos2. *Nat. Nanotechnol.* **2013**, *8*, 497−501.

(14) Wang, H.; Taychatanapat, T.; Hsu, A.; Watanabe, K.; Taniguchi, T.; Jarillo-Herrero, P.; Palacios, T. Bn/Graphene/Bn Transistors For Rf Applications. *IEEE Electron Device Lett.* **2011**, *32*, 1209−1211.

(15) Jena, D. Tunneling Transistors Based On Graphene and 2-D Crystals. *Proc. IEEE* **2013**, *101*, 1585−1602.

(16) Yang, J.; Voiry, D.; Ahn, S. J.; Kang, D.; Kim, A. Y.; Chhowalla, M.; Shin, H. S. Two-Dimensional Hybrid Nanosheets of Tungsten Disulfide and Reduced Graphene Oxide as Catalysts for Enhanced Hydrogen Evolution. *Angew. Chem., Int. Ed.* **2013**, *52*, 13751−13754.

(17) Georgiou, T.; Jalil, R.; Belle, B. D.; Britnell, L.; Gorbachev, R. V.; Morozov, S. V.; Kim, Y.; Gholinia, A.; Haigh, S. J.; Makarovsky, O. Vertical Field-Effect Transistor Based On Graphene-Ws2 Heterostructures for Flexible and Transparent Electronics. *Nat. Nanotechnol.* **2013**, *8*, 100−103.

(18) Roy, K.; Padmanabhan, M.; Goswami, S.; Sai, T. P.; Ramalingam, G.; Raghavan, S.; Ghosh, A. Graphene-Mos2 Hybrid Structures For Multifunctional Photoresponsive Memory Devices. *Nat. Nanotechnol.* **2013**, *8*, 826−830.

(19) Zhang, W.; Chuu, C.; Huang, J.; Chen, C.; Tsai, M.; Chang, Y.; Liang, C.; Chen, Y.; Chueh, Y.; He, J. Ultrahigh-Gain Photodetectors Based on Atomically Thin Graphene-MoS2 Heterostructures. *Sci. Rep.* **2014**, *4*, 3826.

(20) Bertolazzi, S.; Krasnozhon, D.; Kis, A. Nonvolatile Memory Cells based on MoS2/Graphene Heterostructures. *ACS Nano* **2013**, *7*, 3246−3252.

(21) Yoon, J.; Park, W.; Bae, G.; Kim, Y.; Jang, H. S.; Hyun, Y.; Lim, S. K.; Kahng, Y. H.; Hong, W.; Lee, B. H. Highly Flexible and Transparent Multilayer MoS2 Transistors with Graphene Electrodes. *Small* **2013**, *9*, 3295−3300.

(22) Choudhary, N.; Park, J.; Hwang, J. Y.; Choi, W. Growth of Large Scale and Thickness-Modulated MoS2 Nanosheets. *ACS Appl. Mater. Interfaces* **2014**, *6*, 21215−21222.

(23) Das, S.; Sudhagar, P.; Verma, V.; Song, D.; Ito, E.; Lee, S. Y.; Kang, Y. S.; Choi, W. Amplifying Charge-Transfer Characteristics of Graphene for Triiodide Reduction in Dye-Sensitized Solar Cells. *Adv. Funct. Mater.* **2011**, *21*, 3729−3736.

(24) Pimenta, M. A.; del Corro, E.; Carvalho, B. R.; Fantini, C.; Malard, L. M. Comparative Study of Raman Spectroscopy in Graphene and MoS2-type Transition Metal Dichalcogenides. *Acc. Chem. Res.* **2014**, *48*, 41−47.

(25) Li, H.; Zhang, Q.; Yap, C. C. R.; Tay, B. K.; Edwin, T. H. T.; Olivier, A.; Baillargeat, D. From Bulk to Monolayer MoS2: Evolution of Raman Scattering. *Adv. Funct. Mater.* **2012**, *22*, 1385−1390.

(26) Ferrari, A. C.; Basko, D. M. Raman Spectroscopy as a Versatile Tool for Studying the Properties Of Graphene. *Nat. Nanotechnol.* **2013**, *8*, 235−246.

(27) Malard, L.; Pimenta, M.; Dresselhaus, G.; Dresselhaus, M. Raman Spectroscopy in Graphene. *Phys. Rep.* **2009**, *473*, 51−87.

(28) Sundaram, R.; Engel, M.; Lombardo, A.; Krupke, R.; Ferrari, A.; Avouris, P.; Steiner, M. Electroluminescence in Single Layer MoS2. *Nano Lett.* **2013**, *13*, 1416−1421.

(29) Splendiani, A.; Sun, L.; Zhang, Y.; Li, T.; Kim, J.; Chim, C.; Galli, G.; Wang, F. Emerging Photoluminescence in Monolayer MoS2. *Nano Lett.* **2010**, *10*, 1271−1275.

(30) Tongay, S.; Suh, J.; Ataca, C.; Fan, W.; Luce, A.; Kang, J. S.; Liu, J.; Ko, C.; Raghunathanan, R.; Zhou, J. Defects Activated Photoluminescence in Two-Dimensional Semiconductors: Interplay between Bound, Charged, and Free Excitons. *Sci. Rep.* **2013**, *3*, 2657.

(31) Ye, Y.; Ye, Z.; Gharghi, M.; Yin, X.; Zhu, H.; Zhao, M.; Zhang, X. *Exciton-Related Electroluminescence from Monolayer MoS2*; CLEO: Science and Innovations: San Jose, California, United States, 8−13, 2014.

(32) Zhang, W.; Huang, J.; Chen, C.; Chang, Y.; Cheng, Y.; Li, L. High-Gain Phototransistors Based on a CVD MoS2Monolayer. *Adv. Mater.* **2013**, *25*, 3456−3461.

(33) Wu, W.; De, D.; Chang, S.; Wang, Y.; Peng, H.; Bao, J.; Pei, S. High Mobility and High on/off Ratio Field-Effect Transistors Based on Chemical Vapor Deposited Single-Crystal MoS2 Grains. *Appl. Phys. Lett.* **2013**, *102*, 142106.

(34) Dolui, K.; Rungger, I.; Sanvito, S. Origin of the n-Type and p-Type Conductivity of MoS 2 Monolayers on a SiO 2 Substrate. *Phys. Rev. B: Condens. Matter Mater. Phys.* **2013**, *87*, 165402.

(35) Zeng, Z.; Yin, Z.; Huang, X.; Li, H.; He, Q.; Lu, G.; Boey, F.; Zhang, H. Single-Layer Semiconducting Nanosheets: High-Yield Preparation and Device Fabrication. *Angew. Chem., Int. Ed.* **2011**, *50*, 11093−11097.

(36) Zhan, Y.; Liu, Z.; Najmaei, S.; Ajayan, P. M.; Lou, J. Large-Area Vapor-Phase Growth and Characterization of MoS2 Atomic Layers on a SiO2 Substrate. *Small* **2012**, *8*, 966−971.

(37) Tongay, S.; Lemaitre, M.; Miao, X.; Gila, B.; Appleton, B.; Hebard, A. Rectification at Graphene-Semiconductor Interfaces: Zero-Gap Semiconductor-Based Diodes. *Phys. Rev. X* **2012**, *2*, 011002.

(38) Schroder, D. K. *Semiconductor Material and Device Characterization*, 2nd ed.; John Wiley & Sons: New York, NY, 2006.

(39) Cheung, S.; Cheung, N. Extraction of Schottky Diode Parameters from Forward Current-Voltage Characteristics. *Appl. Phys. Lett.* **1986**, *49*, 85−87.

(40) Chuang, S.; Battaglia, C.; Azcatl, A.; McDonnell, S.; Kang, J. S.; Yin, X.; Tosun, M.; Kapadia, R.; Fang, H.; Wallace, R. M. MoS2 P-type Transistors and Diodes Enabled by High Work Function MoO x Contacts. *Nano Lett.* **2014**, *14*, 1337−1342.
(41) Ng, Kwok. K. *Complete Guide to Semiconductor Devices*; J. Wiley & Sons: New York, NY, pp 439−444.
(42) Dawlaty, J. M.; Shivaraman, S.; Strait, J.; George, P.; Chandrashekhar, M.; Rana, F.; Spencer, M. G.; Veksler, D.; Chen, Y. Measurement of the Optical Absorption Spectra of Epitaxial Graphene from Terahertz to Visible. *Appl. Phys. Lett.* **2008**, *93*, 131905.
(43) Casalino, M.; Sirleto, L.; Moretti, L.; Rendina, I. A Silicon Compatible Resonant Cavity Enhanced Photodetector working at 1.55 μm. *Semicond. Sci. Technol.* **2008**, *23*, 075001.
(44) Rumyantsev, S.; Pala, N.; Shur, M.; Gaska, R.; Levinshtein, M.; Adivarahan, V.; Yang, J.; Simin, G.; Khan, M. A. Low-Frequency Noise in Al 0.4 Ga 0.6 N-based Schottky Barrier Photodetectors. *Appl. Phys. Lett.* **2001**, *79*, 866−868.

DOI: 10.1021/acsami.5b00887
ACS Appl. Mater. Interfaces 2015, 7, 15206−15213